

## REPORT DOCUMENTATION PAGE

Public reporting burden for this collection of information is estimated to average 1 hour per response, including the time for reviewing existing information, gathering and maintaining the data needed, and completing and reviewing the collection of information. Send comments regarding this burden estimate or any other aspect of this collection of information, including suggestions for reducing this burden to Washington Headquarters Services, Directorate for Information Operations and Reports, 1215 Jefferson Davis Highway, Suite 1204, Arlington, VA 22202-4302, and to the Office of Management and Budget, Paperwork Reduction Project (0704-0188), Washington, DC 20503.

0201

1. AGENCY USE ONLY (Leave blank)		2. REPORT DATE February 7, 1999		3. REPORT TYPE AND DATES COVERED Final 12/01/97 - 11/30/98	
4. TITLE AND SUBTITLE Structure of Partially Premixed Flames and Advanced Solid Propellants				5. FUNDING NUMBERS PE - 61102F PR - 2308 SA - AX G - F49620-98-1-0069	
6. AUTHOR(S) Melvyn C. Branch and Christopher B. Dreyer					
7. PERFORMING ORGANIZATION NAMES(S) AND ADDRESS(ES) Center for Combustion and Environmental Research Department of Mechanical Engineering University of Colorado at Boulder Boulder, CO 80309-0427				8. PERFORMING ORGANIZATION REPORT NUMBER  CCER Report No. 99-04	
9. SPONSORING / MONITORING AGENCY NAMES(S) AND ADDRESS(ES) Air Force Office of Scientific Research 110 Duncan Avenue, Room B115 Bolling AFB, DC 20332-8050				10. SPONSORING / MONITORING AGENCY REPORT NUMBER	
11. SUPPLEMENTARY NOTES					
a. DISTRIBUTION / AVAILABILITY STATEMENT  Approved for public release; distribution unlimited				12. DISTRIBUTION CODE	
13. ABSTRACT (Maximum 200 words) The combustion of solid rocket propellants of advanced energetic materials involves a complex process of decomposition and condensed phase reactions in the solid propellant, gaseous flame reactions above the propellant surface, and subsequent mixing and flow through the combustion chamber. The response to combustion instabilities is influenced by the structure of the premixed and partially premixed diffusion flames and triple flames at the propellant surface. This research provided experimental data and modeling of partially premixed diffusion flames supported by nitrogen oxides that are common with advanced solid propellants. Of particular interest was the stability and possible extinction of the flames in the presence of velocity fluctuations across the propellant. It was shown that premix flames of highly disparate equivalence ratio can be supported in opposed-flow geometry and will form a triple flame structure. Evidence was presented which indicates that a diffusion flame forms between the premix flames and is due to the conversion of H <sub>2</sub> , O <sub>2</sub> , and CO originating from the premix flame zones to H <sub>2</sub> O and CO <sub>2</sub> .					
14. SUBJECT TERMS  Solid Propellant Combustion				15. NUMBER OF PAGES	
				16. PRICE CODE	
17. SECURITY CLASSIFICATION OF REPORT unclassified		18. SECURITY CLASSIFICATION OF THIS PAGE unclassified		19. SECURITY CLASSIFICATION OF ABSTRACT unclassified	
				20. LIMITATION OF ABSTRACT  UL	



**Center for  
Combustion and  
Environmental  
Research**

## **Structure of Partially Premixed Flames and Advanced Solid Propellants**

(From 1 December 1997 to 30 November 1998)

**M.C. BRANCH AND C.B. DREYER**

*Center for Combustion and Environmental Research  
Department of Mechanical Engineering  
University of Colorado, Boulder, CO 80309-0427, USA  
Tel: 303-492-7247  
Fax: 303-492-2199  
Email: [branch@spot.colorado.edu](mailto:branch@spot.colorado.edu)*

**FINAL TECHNICAL REPORT  
AFOSR GRANT NO. F49620-98-1-0069**

**CCER Report No. 99-04**

**19990823 146**



## EXECUTIVE SUMMARY

The combustion of solid rocket propellants of advanced energetic materials involves a complex process of decomposition and condensed phase reactions in the solid propellant, gaseous flame reactions above the propellant surface, and subsequent mixing and flow through the combustion chamber. The response to combustion instabilities is influenced by the structure of the premixed and partially premixed diffusion flames and triple flames at the propellant surface (See Figure 1). The research has provided experimental data and modeling of partially premixed diffusion flames supported by nitrogen oxides that are common with advanced solid propellants. Of particular interest was stability and possible extinction of the flames in the presence of velocity fluctuations across the propellant.

Steady, laminar triple flames established in an opposed flow flame facility were studied in detail to obtain major and minor species concentration profiles and flow visualization. These results were compared to detailed flame modeling results. This has enabled the development of appropriate reduced kinetic mechanisms for such flames. Conditions ranging from near-equilibrium or fast chemistry, to near-extinction situations were studied.

It was shown that premixed flames of highly disparate equivalence ratio can be supported in opposed-flow geometry and will form a triple flame structure. Evidence was presented which indicates that a diffusion flame forms between the premixed flames and is due to the conversion of  $H_2$ ,  $O_2$ , and CO originating from the premixed flame zones to  $H_2O$  and  $CO_2$ .

The experimental studies were conducted in a new flame chemistry laboratory that has been constructed for the Center for Combustion and Environmental Research at the University of Colorado at Boulder. The diagnostics for the measurement include an existing Excimer pumped dye laser and a new Nd-Yag pumped dye laser system with a CCD camera for 2D fluorescence imaging and Rayleigh and Raman measurements obtained in 1997 through a Defense University Research Instrumentation grant.

## PUBLICATIONS

J.J. Cor, C.B. Dreyer, and M.C. Branch, "Mechanistic Studies of Low Pressure Flames Supported by Nitrogen Oxides," *Challenges in Propellants and Combustion 100 Years after Nobel*, K.K. Kuo, Ed., Begell House, New York, pp. 70-80, 1997.

J.J. Cor and M.C. Branch, "Studies of Counterflow Diffusion Flames at Low Pressure," *Combustion Science and Technology*, 127, pp. 71-78, 1997.

M.C. Branch, "Propellants and Combustion," *Aerospace America*, 35, p. 67, 1998.

## STUDENT SUPPORT

Christopher Dreyer, PhD Candidate, expected graduation date, December 1999

## LOW PRESSURE FLAME FACILITY

The counter flow premixed flames were studied in the facility developed for low pressure laminar flame studies. This facility has been used successfully for a number of different studies [Cor, 1995; Mallik, 1994]. The facility consists of two opposed burner surfaces from which fuel and oxidizer emanate. The burner is housed in a chamber and attached a translation stage. Optical access of the burner is available from four sides. Figure 2 is an illustration of the counterflow burner. The two burner housings are positioned opposite to each other and oriented vertically. The housings are manufactured from stainless steel and have been machined for gas entry ports, for the attachment of the burner surface, and for securing a dividing porous plate within the housing. Gas flows into a small open space at the bottom of the burner (the lower burner is used in this discussion, the upper burner is identical). The gas then flows through a porous metal plate into a cavity containing a packed bed of glass beads. The gas flows through the glass beads to the 1 cm thick ceramic honeycomb burner surface. The burner surface is 67.0 mm in diameter. The housings are 75 mm from surface to base. The burner housing consists of two parts that screw into each other. The upper part is a ring that holds the ceramic burner surface in place tightly against the bed of glass beads. This combination of porous metal plate, glass beads, and ceramic honeycomb burner surface was designed to insure that the flow out of the burner is laminar and uniform, and to prevent flashback.

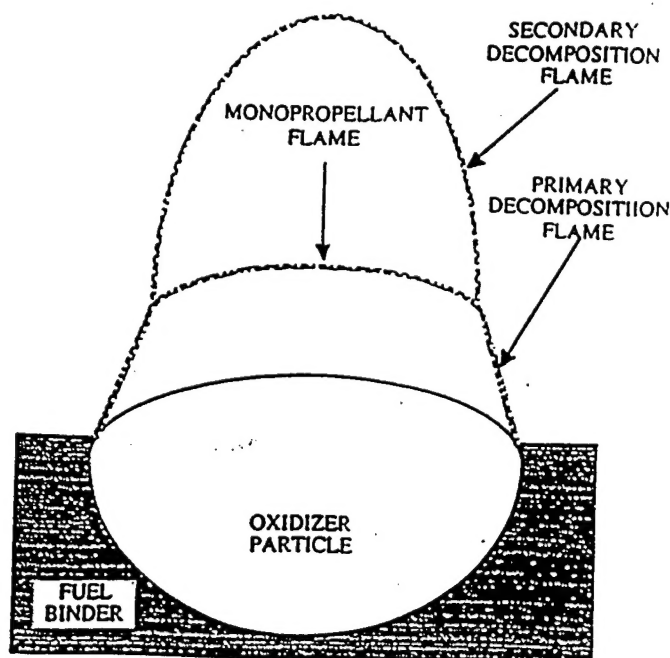
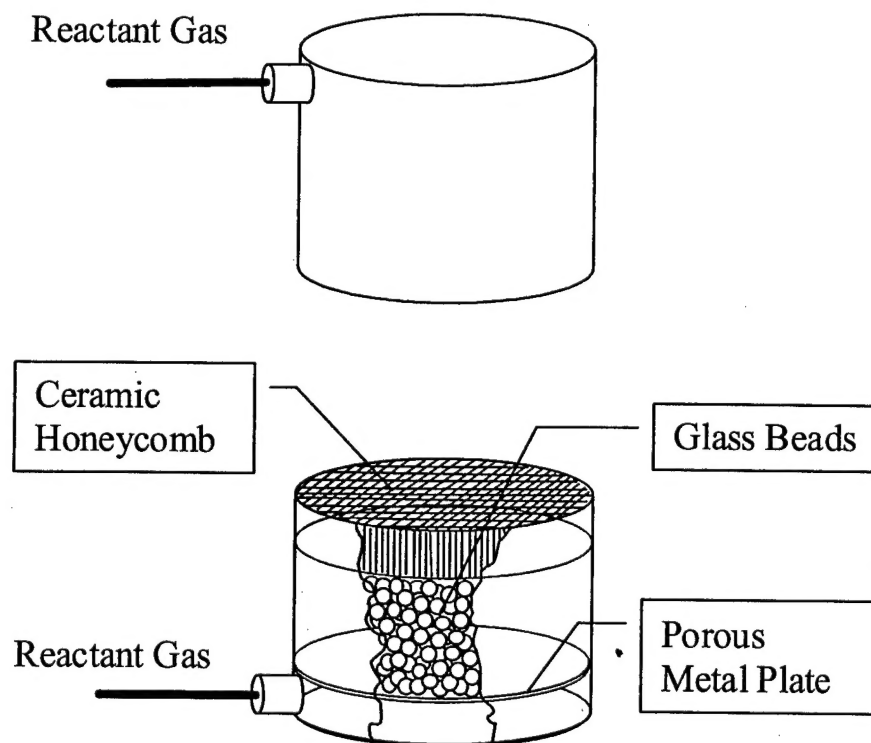
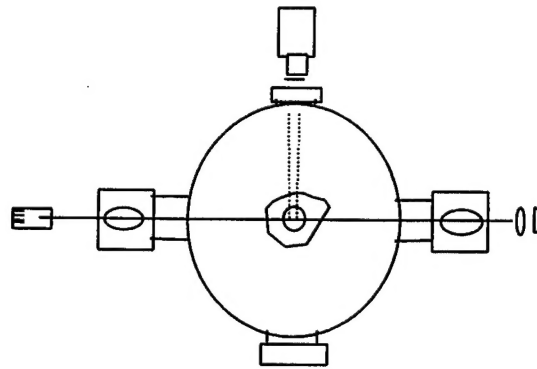


Figure 1. A solid rocket propellant is composed of a matrix of oxidizer particles of varying sizes and more-or-less spherical shape which are bound together by a fuel binder. During a rocket firing, each oxidizer particle burns with a portion of the binder which surrounds it, forming partially premixed gaseous flames in which fuel molecules react with nitrogen containing oxidizers.

The burners are fixed in place in a rigid aluminum frame. The lower burner is attached to a high quality lab jack. The separation distance with the current set up can be varied from nearly 0 cm to 2.48 cm, but the range could easily be increased. The burner frame is situated in the center of the chamber on a translation stage. The frame is attached to a support stand that is fed through the bottom to the chamber and attached to two stepper motors. The stepper motor assembly enables vertical (resolution 0.01 mm) and radial articulation of the burner frame. Optical access is provided from four sides, (see Figure 3). On two sides, the windows have been placed at a 30 degree angle (approximately the Brewster angle for an air-quartz interface) to minimize laser beam transmission loss. Perpendicular to the Brewster windows, are two vertical windows. One is used for manual access of the burner (needed to ignite the flame), the other for viewing fluorescence. The Brewster angle windows and the fluorescence viewing window are Quartz, while the window for manual access is Pyrex.



**Figure 2 Counterflow Burner**



**Figure 3** Optical access of Low Pressure Flame Facility

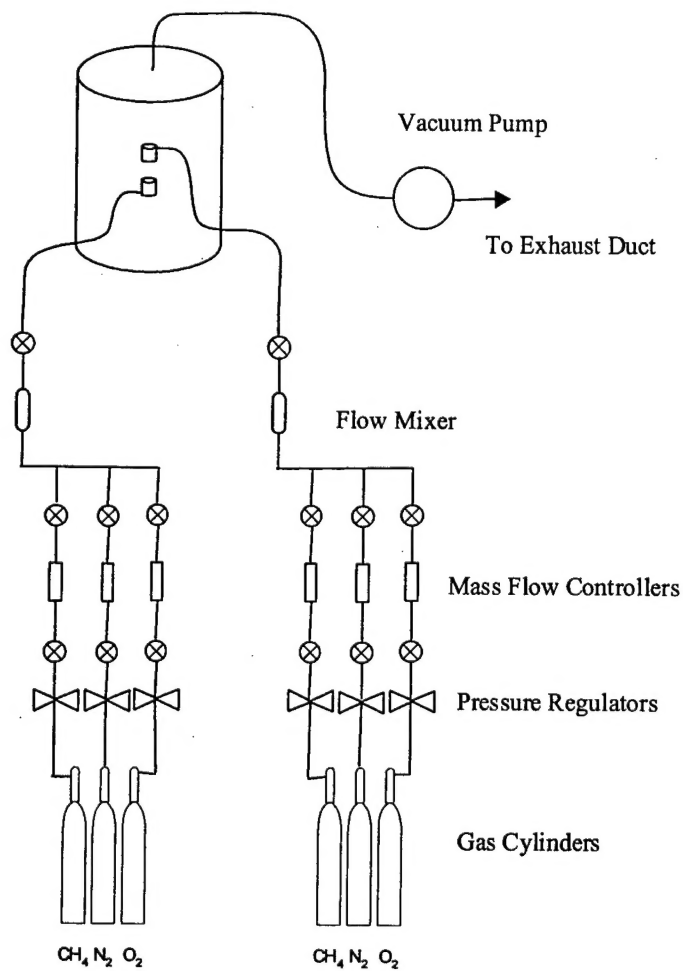


**Figure 4** Schematic of gas flow system of the low pressure facility, configured for counter flow premixed flames.

Low pressure is maintained in the chamber by a vacuum pump. The minimum pressure achievable is dependent on flow conditions, but it is typically between 20 and 100 torr. Gases are fed to the chamber through a set of mass flow controllers, gasses supplied from high pressure cylinders (see Figure 4). The chamber is 44 cm diameter and 69 cm tall.

After passing through the mass flow controllers the gases are directed into two streams. Each gas stream flows through separate flow mixers. The flow mixers ensure that the reactants are thoroughly premixed before reaching the chamber. The flow mixers also serve as back-up flame arrestors, although, as mentioned earlier, the burners have been designed with flame arrestment in mind. The doubly safe design makes it very unlikely that a hydrocarbon mixture would flash back through the feed lines to the high pressure cylinders. Mass flow controllers are calibrated with a Precision Scientific Wet Test Gas Meter, cat. no. 63111. Pressure in the chamber is measured with an Omega PX176 0-15 psia pressure transducer. The pressure measurement is displayed in units of psia on an Omega LCD read-out box.

In addition to measurement using LIF, temperature is measured in the flame with a radiation corrected Pt-Pt/13% Rh thermocouple. The thermocouple is protected from the combustion products by an aluminum oxide shroud, the shroud also serves as the support to extend the thermocouple into the reaction zone. A protective coating of ceramic bonding material, Ceramabond 569, is applied to the thermocouple junction. This protection is required to prevent the thermocouple wire from oxidizing in the flame and to prevent catalytic reactions on the wire surface. The thermocouple wires run to a ceramic-insulated junction inside the combustion chamber, which is connected to insulated wires which run out of the combustion chamber to a meter which displays the thermocouple temperature in degrees Kelvin. Measurements are taken at intervals between the burner surfaces by translation of the burner frame using the stepper motor. Thermocouple measurements are corrected for radiation losses to the chamber walls.

## FLAME MODELING TOOLS

Reacting flows in a counterflow geometry were modeled with the computer code OPPDIF, developed by Lutz et al. [Lutz et al. 1997]. The code uses the Chemkin set of subroutines to compute species thermodynamic properties and transport properties using a full multi-component formulation. The problem is reduced to a one-dimensional boundary value problem in which the radial pressure gradient is treated as an eigenvalue. A second-order accurate spatial finite difference discretization of the governing equations leads to a set of algebraic equations that is solved using a damped modified Newton algorithm. If the Newton algorithm fails to converge, the solution estimate is conditioned by a period of time integration, which supplies a new starting estimate for the Newton algorithm. Grid refinement is used to resolve the solution to the desired accuracy. Generation rates of individual species due to individual reactions and sensitivity values are computed for chemical mechanism analysis. Chemical kinetic mechanisms that are used in this study are the mechanism developed by Branch and Cor, and the GRI mechanism [Bowman, 1997].

## PLIF EXCITATION/DETECTION SCHEMES

Laser-induced fluorescence is a complicated diagnostic technique. Correct application of PLIF requires knowledge of molecular transition probability, molecular structure, laser design, camera design, and much more. This section outlines the detection scheme used in this work.

The experimental arrangements needed for PLIF of each of the transitions considered in this work are presented in Table 1. The table includes the laser pump transitions for each molecule in this study, the laser dye and frequency doubler combination needed to produce the pump beam, and estimated maximum energy per pulse of the beam, as well as the fluorescence detection band.

Pump Transition	Yag Pump (nm)	Laser Dye (and frequency doubler combination)	Maximum Laser Output (mJ)	Detection Band
CH , near 435 nm $A^2\Delta \rightarrow X^2\Pi (0,0)$ P or Q branch near $J'' = 7$	355	C440	32	Same
HCO , near 258 nm $B^2A'-X^2A' (0,0,0)$ $^Q R_0(9)$ and $^R Q_0(7)$	355	R610 + freq. Double	0.78	Same
	532	KR620 + freq. Double	3.5	Same

**Table 1** Summary of the laser configuration options for molecules proposed.

There are sufficient data in the literature to predict the CH saturation laser irradiance, this was done and estimates place it at  $3.4 \text{ W}/(\text{cm}^2\text{sec}^{-1})$ . Assuming a 2 cm by 100  $\mu\text{m}$  laser sheet, the required laser power is 0.4  $\mu\text{J}$ . Resonance fluorescence is suggested for CH and HCO PLIF. Signal strength estimates of the CH pump-detection scheme predict single shot PLIF of CH is possible in the linear regime. As the pump laser power is increased the scattered Rayleigh signal increases and over takes the fluorescence signal. Diau et al. (1998) indicate that in a stoichiometric methane-air, 25 Torr, the saturation irradiance of HCO was 25  $\mu\text{J}$ . Thus, HCO saturation should be attainable when pumping in the 355 nm arrangement. Because of Rayleigh scatter, saturation is not desirable, but it is desirable to maximize the signal while still within the linear range.

Einstein coefficients for emission and absorption are available for CH. Some emission and absorption cross section data are available for HCO, but the information

falls short of what is needed. Quenching data for CH, and to a lesser extent HCO, are available. With the computer-modeled mole fractions for major species and measured temperature data it is possible to fully correct PLIF images of CH and HCO. An important part of this correction was determination of uncertainty in the corrected measurement.

PLIF imaging requires 4 image sets for each flame:

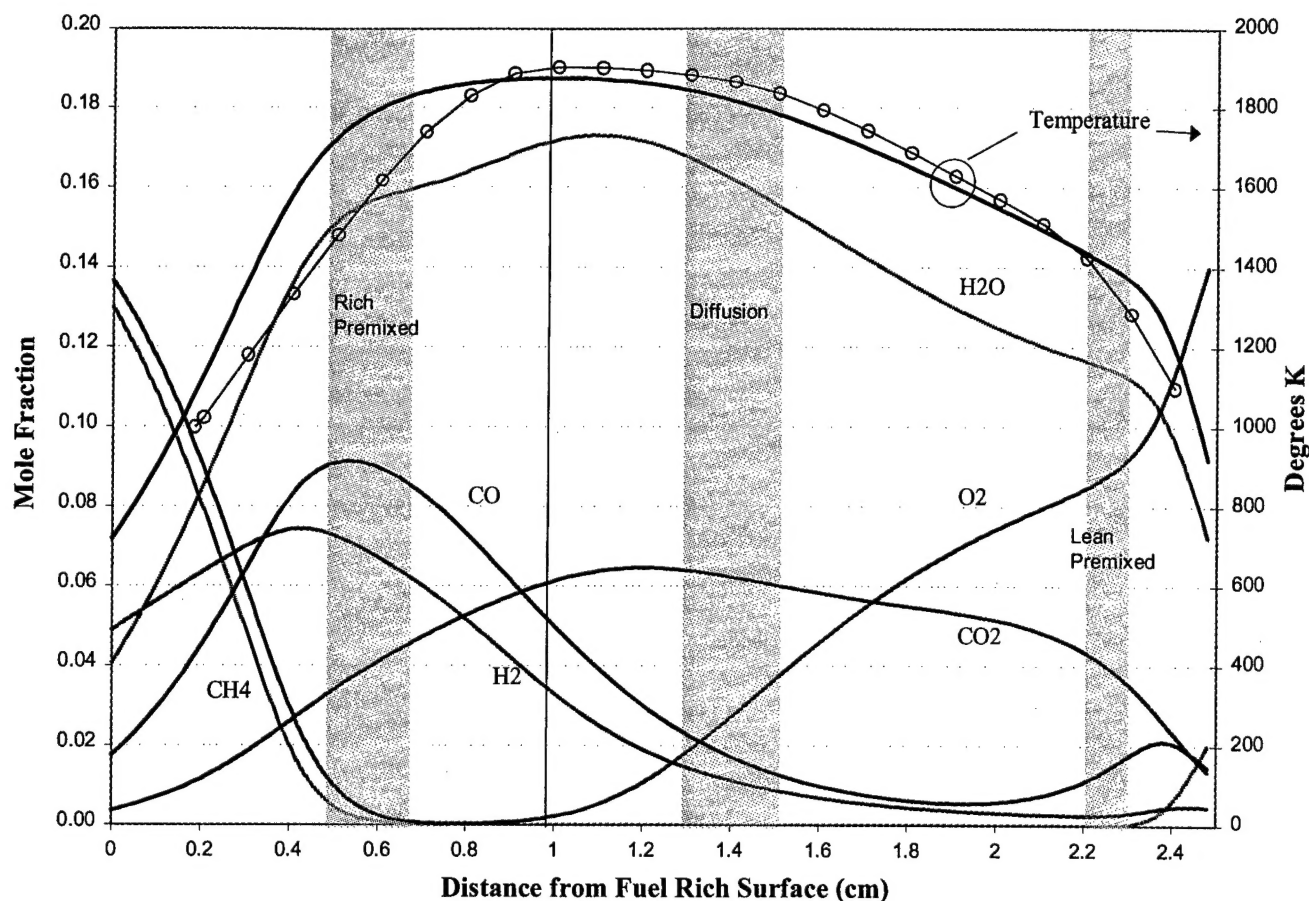
- 1) Uniform illumination of camera (no flame, no laser).
- 2) Room-temperature Rayleigh image of air (no flame).
- 3) Hot Rayleigh image, laser tuned off absorption line (in flame).
- 4) PLIF image of target molecule (in flame).

Image 1 provides pixel gain and intensifier error pattern correction. Rayleigh image 2 provides correction of laser intensity variation in the image plane. Rayleigh image 3 provides background Rayleigh and emission subtraction for correction of PLIF image. An added bonus of this plan is that the ratio of Rayleigh image 2 to Rayleigh image 3 provides a direct image of the temperature field. Uncertainty in this measurement is dependent on the Rayleigh cross-section and originates from the uncertainty in the flame model prediction of major species. Multiple images of each of the 4 sets are required for each operating condition and used to estimate system noise.

### TRIPLE FLAME WORK

The objectives of the triple flame work were to observe and model the structural changes in a disparate counterflow premixed flame as the strain rate is increased toward the quenching limit. The flame had reactant flows of  $\phi_{\text{rich}} = 1.5$  and  $\phi_{\text{lean}} = 0.5$ . As the extinction strain rate for this flame is not known some preliminary experiments were performed to determine the burner separation distance, mass flow controller, and burner surface design needed to attain the extinction strain rate.

In earlier studies, [Cor, 1996] a few simple experiments with the low pressure flame facility were conducted to determine if triple flames could be observed in the apparatus. Cor noted the visible structure and measured the temperature profile of three flames. Experimental temperature data and computed temperature and species data for the methane-air flame Cor studied are presented in Figure 5.



**Figure 5** Experimental and numerical results of methane-air triple flame studied by Cor (1996);  $\phi_{\text{rich}} = 2.04$ ,  $\phi_{\text{lean}} = 0.56$ ,  $v_{\text{rich}} = 34.0$  cm/s,  $v_{\text{lean}} = 58.9$  cm/s,  $P = 0.167$  atm,  $a = 38$  s<sup>-1</sup>. Solid lines are computed mole fractions using Branch-Cor mechanism. Radiation corrected thermocouple measurements are shown with open circles. Gray vertical bars indicate the observed locations of the visible flames. Vertical line at 0.98 cm is stagnation surface.

The flame of Figure 5 had three visible flame zones, indicated by the gray vertical bars. The temperature profile of this flame was measured by a thermocouple. The radiation-corrected thermocouple measurements are plotted along with the computed temperature and major species profiles. The computation was run with the Branch-Cor mechanism with the energy equation included. The only experimentally determined values in the computation are the burner surface temperatures, burner surface velocities, and initial burner surface species concentrations. It is readily apparent that in the flame of Figure 5, there is significant heat loss to the burners. At both burner surfaces the temperature is great enough for significant conversion of reactants to products. Both premixed flames are very close to the burner surfaces so that diffusion of products to the burner surfaces occurs. The reactant mixture from each surface is very close to the lean flammability limit of methane-air ( $\phi = 0.53$ ), and beyond the rich flammability limit ( $\phi = 1.58$ ) [Kuo, 1986]. Cor [1996] observed that this flame was not very stable and, had a

tendency to blow out after an hour of operation with no apparent change in conditions. The observed locations of the premixed flame zones appear to be further from the burner surface than the computed locations, particularly the lean premix flame zone. This could be due to the inherent difficulty of measuring the gas temperature at the burner surface, which is needed as a boundary condition for the flame code. The temperature gradients at the burner surface are high. The temperature cannot be measured directly at the surface because of the ceramic honeycomb surface. Surface temperatures were estimated from the temperature gradient measured just upstream of the burner exits.

The premixed flames located themselves such that the local gas velocity matched the laminar flame speed. Since it was apparent that the flames suffered from significant heat loss to the burners, the local gas velocity must be lower than the laminar flame speed of the mixture. The laminar flame speed ( $S_l$ ) increases with decreasing pressure for hydrocarbon-air mixtures [Kuo, 1986]. Laminar flame speeds of premixed flames have been measured at various pressures [Egolfopoulos et al., 1989]. Egolfopoulos et al. [1989] observed that the relationship of laminar flame speed to equivalence ratio ( $\phi$ ) is a bell shaped curve, centered near  $\phi = 1.1$ , with a peak value of 61 cm/s, at  $\phi = 0.7$  to be 36 cm/s, and at  $\phi = 1.5$  to be 44 cm/s at 0.25 atm. The reactant mixtures studied by Cor [1996] were leaner and richer respectively than the data from Egolfopoulos et al. [1989], but if the trend can be extrapolated,  $S_l$  is approximately 25 cm/s at  $\phi = 0.58$  and approximately 20 cm/s at  $\phi = 2.0$ . Thus, the surface velocities for the flame studied by Cor were much higher than the estimated laminar flame speed of the same mixture.

Opposed flow premixed flames have two stable locations in the flow if the burner exit velocity is greater than the laminar flame speed. In the opposed flow geometry the axial velocity decreases away from the burner surface, reaching zero at the stagnation plane. If the exit velocity is greater than the laminar flame speed of an adiabatic flame, then the flame can locate close to the burner surface where heat loss to the burner is lower than the effective flame speed of the mixture (non-adiabatic flame). The flame can also locate itself at a point between the burner surface and the stagnation surface where the local gas velocity is reduced to the adiabatic flame speed by flow divergence.

In the work by Cor [1996], it appears that the flame was anchored to the burner surface, and so is non-adiabatic. In all of the work on strained laminar flames, except Hou [1991], the flames locate themselves between the burner surface and the stagnation plane. The majority of studies examine adiabatic flames. If one is to provide meaningful information to turbulent combustion modelers, it is best to obtain data on strained adiabatic flames. Heat loss is difficult to quantify, and at this point in the debate over flamelet theory and turbulent combustion modeling it is an unnecessary complication.

For these reasons, two additional computations were made. The surface temperature was fixed at a 430K, the burner separation distance was increased to 3.5 cm, and the reactant mixture mole fraction changed. Results are plotted in Figures 6 and 7. The two flames presented in Figures 6 and 7 show that the flames are not anchored to the burner surface and have taken a position roughly halfway between the burner surface and the stagnation plane. Heat loss to the burner is negligible (as judged by the zero temperature gradient), however, as the gas temperature at the burners was chosen as 430 K, the gases are slightly preheated. The gas exit velocity in Figure 6 is 90 cm/s and 115

cm/s in Figure 7. The effect of different flow velocities can be seen in that the premixed flames of Figure 7 are pushed closer to the stagnation surface than the flame of Figure 6.

From Figures 5, 6, and 7, the triple flame structure is revealed. In all of these flames the rich premixed flame consumes all of the fuel. If this premixed flame was not interacting with other flames, excess fuel would pass through the flame. In fact, in high activation energy asymptotic models of triple flames by C. K. Law [Sohrab et al., 1986], the excess fuel of the rich premixed flame does pass through the flame. They observe a diffusion flame in the asymptotic model that is due to reaction between excess fuel from one side, and excess oxygen from the other. From the work by Cor [1996] and the modeling presented here,

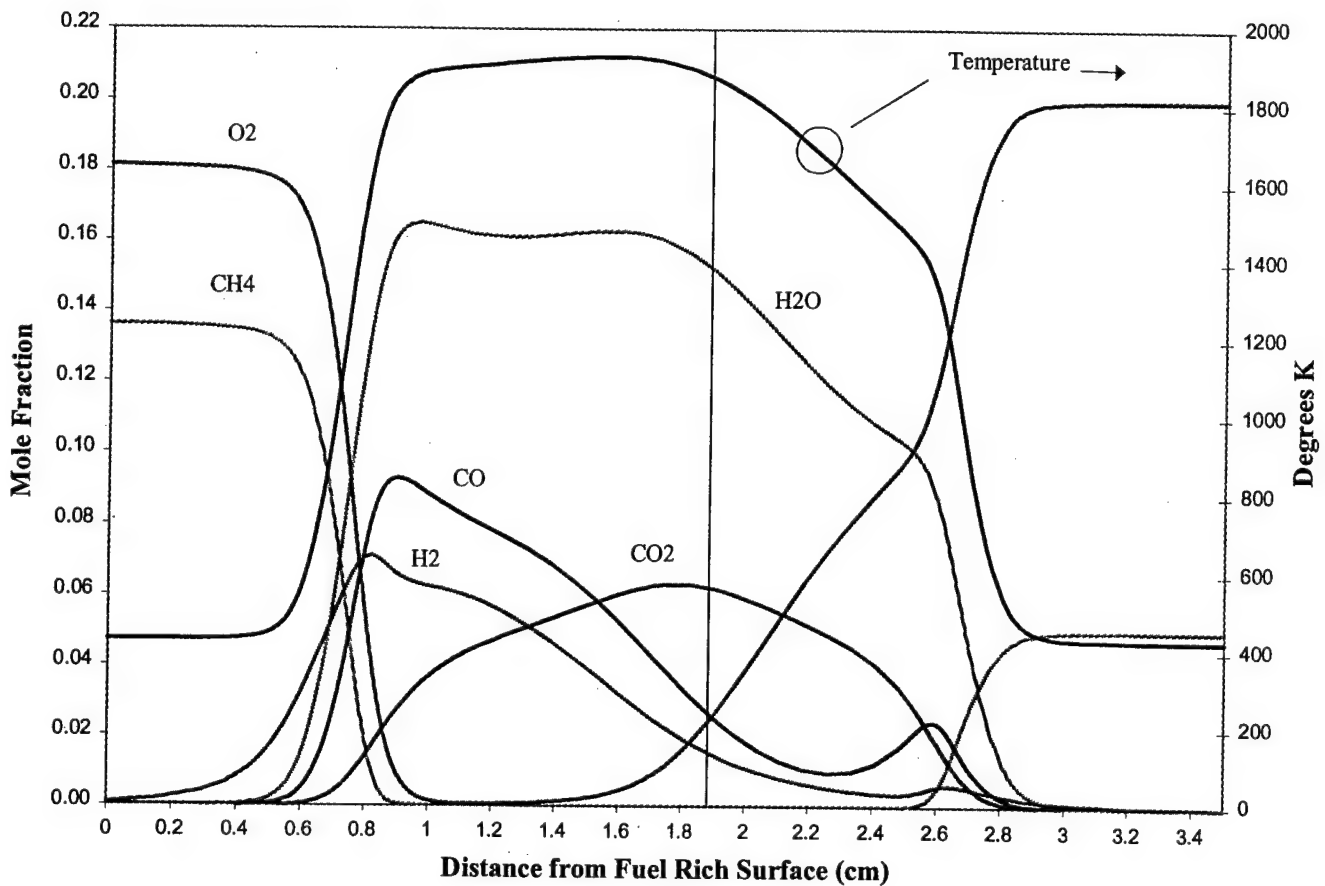


**Figure 6** Numerical results of methane-air triple flame;  $\phi_{\text{rich}} = 1.5$ ,  $\phi_{\text{lean}} = 0.5$ ,  $v_{\text{rich}} = v_{\text{lean}} = 90$  cm/s,  $P = 0.167$  atm,  $a = 51$  s<sup>-1</sup>. Solid lines are computed mole fractions using Branch-Cor mechanism. Vertical line at 1.88 cm is stagnation surface.

it appears that the chemistry of the rich premixed flame was altered by the presence of the other flames such that all of the methane was consumed in the premixed flames. The diffusion flame appeared to be a reaction between CO and H<sub>2</sub> products of the rich premixed flame and excess oxygen from the lean premixed flame. This chemistry has been observed by others, Echekki and Chen [1997], who performed DNS modeling of a

methanol-air triple-flame (of the type first observed by Philips [1965]). Echekki and Chen used a  $C_1$  chemical mechanism and found the diffusion flame to be due to the consumption of CO and  $H_2$ , produced in the rich branch, with unreacted  $O_2$  from the lean branch.

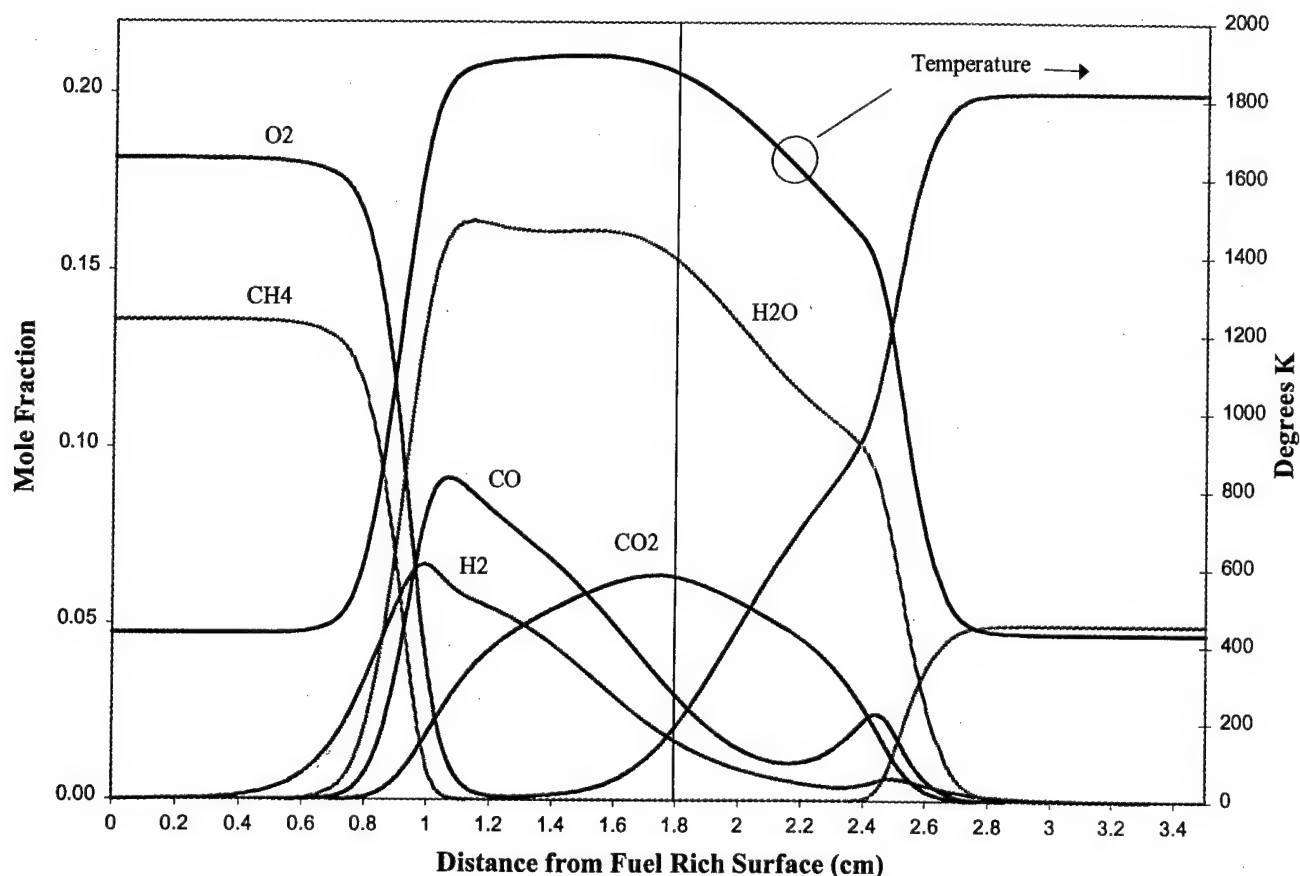


**Figure 7** Numerical results of methane-air triple flame;  $\phi_{rich} = 1.5$ ,  $\phi_{lean} = 0.5$ ,  $v_{rich} = v_{lean} = 115$  cm/s,  $P = 0.167$  atm,  $a = 66$  s $^{-1}$ . Solid lines are computed mole fractions using Branch-Cor mechanism. Vertical line at 1.80 cm is stagnation surface.

The characteristic strain rate,  $a$ , of all flames studied thus far was very low (38, 51 and 66 s $^{-1}$ ) compared to the extinction strain rates of comparable flames. There are no studies of strained flames with reactant stoichiometry identical to those examined in this study. The nearest studies to date are of identical opposed premixed flows at atmospheric pressure. These studies can be useful to make rough estimates of the extinction strain rate for the disparate opposed premixed flows. Identical opposed premixed flames with  $\phi$  near stoichiometric have been studied by a number of researchers; [Sun et al., 1996; Law et al., 1994; Tanoff et al., 1996; Sung et al., 1996]. The majority of the work in the references cited do not experimentally examine flames near extinction. The authors often cite difficulty in attaining the high flow rates necessary to attain extinction. The work by these researchers indicate that the characteristic extinction strain rate is around 400 s $^{-1}$

near stoichiometric, less than  $150 \text{ s}^{-1}$  for equivalence ratios near the extremes ( $\phi=0.5$  and  $\phi=1.5$ ).

All of the studies cited were carried out at atmospheric pressure. It is expected that the extinction strain rate is proportional to the laminar flame speed. The overall reaction order of hydrocarbon-air is greater than one, usually cited as being 2 or 3 for most hydrocarbons. Egolfopoulos et al. [1989] measured laminar flame speeds of methane-air flames from 3 to 0.25 psi. Their work indicates that there is roughly a factor of two increase in laminar flame speed as the pressure goes from 1 atm to 0.25 atm. As a rough, first estimate, the extinction flame rates of low pressure premixed flames may be as much as 4 times greater than rates measured.

The primary use of PLIF is to locate the flame zones. In one-to-one imaging the camera has 85 microns resolution. With this resolution, nearly 150 data point can be collected from one burner surface to the other. In addition, PLIF images provide a quick check of edge effects, a potential problem often ignored in counter flow studies.

Much more spectroscopic data are available for CH, and it is often cited as a reliable measure of flame location and heat release [Eckbreth, 1996]. However, in a recent report by a group at Sandia National Labs, Najm et al. [1998], CH PLIF was determined not to be a good measure of flame location and heat release. The authors have studied numerically and experimentally the impingement of a vortex pair on a laminar flame sheet. They examined many different measurable flow-chemical parameters and found that HCO tracks the flame zone well over a large range of conditions. The authors also demonstrate PLIF of HCO. The counterflow flame of Figure 7 was examined to determine if CH would be a reliable measure of flame location. The results are displayed in Figure 8.

In Figure 8 the computed mole fractions of HCO and CH are compared to the computed temperature gradient,  $|dT/dx|$ . The proper comparison is with heat release. Temperature gradient was used because it is readily extractable from the flame code. The temperature gradient is expected to be broader and located closer to the burner surface than the location of the flame because of thermal diffusion. Several flame radicals were considered:  $\text{CH}_3$ ,  $\text{CH}_2$ ,  $\text{C}_2$ , and OH. All but OH showed a local maximum in the premixed flames, but only HCO and  $\text{CH}_3$  displayed peaks of comparable strength. The hydroxyl radical, OH, may be an interesting radical to measure in these flames, but it is long lived and is present in high concentration between the premixed flames. The dynamic range of PLIF is smaller than other laser diagnostic techniques. If a radical is to mark the premixed flames the peak heights must be within an order of magnitude. From Figure 8 it is clear that HCO meets the necessary criterion, while CH does not.

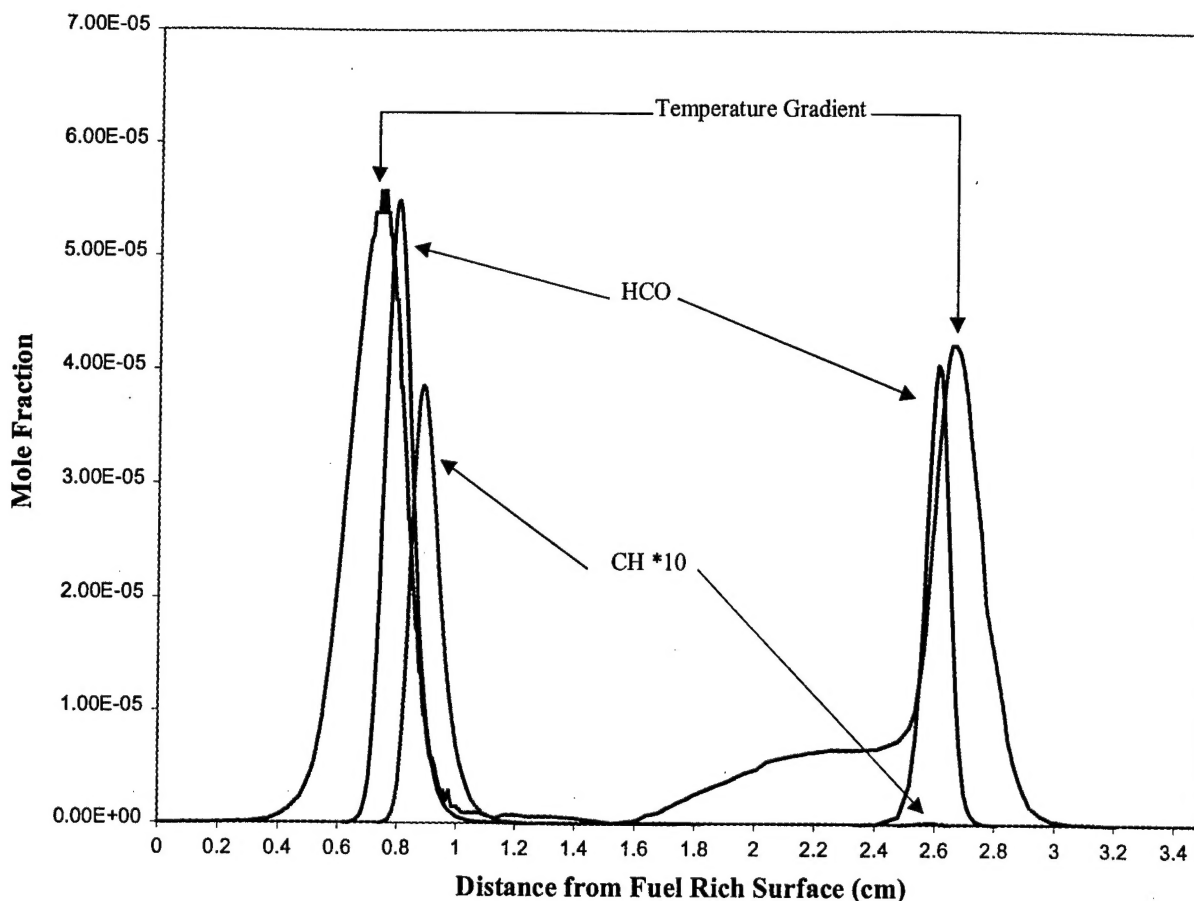


**Figure 8** Comparison of HCO and CH computed mole fractions to computed temperature gradient. Methane-air triple flame;  $\phi_{\text{rich}} = 1.5$ ,  $\phi_{\text{lean}} = 0.5$ ,  $v_{\text{rich}} = v_{\text{lean}} = 90$  cm/s,  $P = 0.167$  atm,  $a = 51$  s<sup>-1</sup>, burner surface temperature fixed at 430 K.

The group at Sandia National Lab, Najm et al. [1998], demonstrated HCO PLIF by excitation of the HCO B-X (0,0,0)  $^2Q_0(9)$  and  $^2Q_0(7)$  near 258.39 nm, pump beam power of 10 mJ, image size 2 cm by 250  $\mu\text{m}$ . They had to average 100 laser shots to obtain a usable PLIF image. The Yag laser system is capable of this pumping strategy, although not this beam energy, however, averaging of 100 shots or more is not a problem because of the steady nature of the flame. PLIF of CH should not be disregarded. Much more spectroscopic data is known about CH than HCO. Also, the suggestion that CH is not an ideal measure of flame location is an interesting idea worthy of investigation.

As for locating the diffusion flame, modeling indicates that no radical species accessible by LIF are present in this flame. Emission from Bunsen-type flames is due to  $\text{CH}^*$ ,  $\text{C}_2^*$ ,  $\text{CO}_2^*$  and  $\text{OH}^*$  (the \* indicates an electronically excited state). The electronically excited radicals are generated by chemical reactions in the flame. It is interesting that  $\text{CO}_2^*$  is responsible for some visible emission, as the diffusion flame observed was located in a region where model results indicated that  $\text{CO}_2$  was being created by reaction of CO and  $\text{H}_2$ .

## LIST OF REFERENCES

- C. T. Bowman, R. K. Hanson, W. C. Gardiner Jr., V. Lissianki, M. Frenklach, M. Goldenberg, and G. P. Smith, "GRI - Mech - An Optimized Detailed Chemical Reaction Mechanism for Methane Combustion and NO Formation and Reburning," GRI Report 97-0020. Refer to the GRI - Mech homepage at <http://www.me.berkeley.edu/gri-mech/>.
- J. J. Cor, *The Structure of Methane-Oxygen, Methane-Nitrous Oxide and Carbon Monoxide-Nitrous Oxide Diffusion Flames at Low Pressures*, Ph.D. Dissertation, University of Colorado at Boulder, 1995,
- J. J. Cor, Report on Preliminary Investigations into the Structure of Triple Flames at Low Pressures, unpublished, 1996.
- E. Diau, G. Smith, J. Jefferies, and D. Crosley, Laser-Induced Fluorescence of HCO Concentration in Flames; AIAA 98-0154.
- T. Echekki and J. H. Chen, Structure and Propagation of Methanol-Air Triple Flames; Western States Section of the Combustion Institute, 1997 Spring Meeting.
- A. C. Eckbreth, *Laser Diagnostics for Combustion Temperature and Species*, 2nd ed., Gordon and Breach Pub, United Kingdom, 1996.
- F. N. Egolfopoulos, P. Cho, and C. K. Law, Laminar Flame Speeds of Methane-Air Mixtures Under Reduced and Elevated Pressures; *Combust. Flame* **76**, 375-391 (1989).
- S. S. Hou, C. K. Chang and T. H. Lin, An Experimental Investigation on Multiflame Burning Structure in Conserved Systems; *Combust. Sci. and Tech.* **79**, 35-48 (1991).
- K. Kuo, *Principles of Combustion*, John Wiley & Sons, New York, 1986
- C. K. Law, C. J. Sung, G. Yu and R. L. Axelbaum, On the Structural Sensitivity of Purely Strained Planar Premixed Flames to Strain Rate Variations; *Combust. Flame* **98**, 139-154 (1994).
- A. E. Lutz, R. J. Kee, J. F. Grcar, and F. M. Rupley, *OPPDIF: A Fortran Program for Computing Opposed-Flow Diffusion Flames*, Sandia Report, SAND96-8243, 1997.

S. Mallik, *Combustion Chemistry of Fuel Additives for Reduced Engine Emission*, MS Thesis Dissertation, University of Colorado at Boulder, 1994.

H. N. Najm, P. P. Paul, C. J. Mueller, P. S. Wyckoff, On the Adequacy of Certain Experimental Observables as Measurements of Flame Burning Rate; *Combust. Flame* **113**, 343-360 (1998).

H. Phillips, Flame in a Buoyant Methane Layer; Tenth Symposium (International) on Combustion, The Combustion Institute, Pittsburgh, 1965, 1277-1283.

S. H. Sohrab, Z. Y. Ye and C. K. Law, Theory of Interactive Combustion of Counterflow Premixed Flames, *Combust. Sci. and Tech.* **45**, 27-45 (1986).

C. J. Sun, C. J. Sung, D. L. Zhu and C. K. Law, Response of Counterflow Premixed and Diffusion Flames to Strain Rate Variations at Reduced and Elevated Pressures; Twenty-Sixth Symposium (International) on Combustion, The Combustion Institute, Pittsburgh, 1996, 1111-1120.

C. J. Sung, J. B. Liu and C. K. Law, On the Scalar Structure of Nonequidiffusive Premixed Flames in Counterflow; *Combust. Flame* **106**, 168-183 (1996).

C. J. Sung and C. K. Law, Extinction Mechanisms of Near-Limit Premixed Flames and Extended Limits of Flammability; Twenty-Sixth Symposium (International) on Combustion, The Combustion Institute, Pittsburgh, 1996, 895-873.

M. A. Tanoff, M. D. Smooke, R. J. Osborne, T. M. Brown and R. W. Pitz, The Sensitive Structure of Partially Premixed Methane-Air vs. Counterflow Flames; Twenty-Sixth Symposium (International) on Combustion, The Combustion Institute, Pittsburgh, 1996, 1121-1128.

W1

AIR FORCE OFFICE OF SCIENTIFIC  
RESEARCH (AFOSR)  
NOTICE OF TRANSMITTAL TO DTIC. THIS  
TECHNICAL REPORT HAS BEEN REVIEWED  
AND IS APPROVED FOR PUBLIC RELEASE  
IWA AFR 190-12. DISTRIBUTION IS  
UNLIMITED.  
YONNE MASON  
STINFO PROGRAM MANAGER